Engineering Symposium at Bánki
(ESB 2025)

Altered Spatiotemporal Muscle Synergies in Chronic Ankle Instability: Evidence of Proximal Compensatory Strategies During Landing

[1]Tianle Jie, [2]Tibor Goda

[1]Obuda University, Doctoral School on Safety and Security Sciences, Budapest, Hungary, JieTianle@stud.uni-obuda.hu
[2]Obuda University, Doctoral School on Safety and Security Sciences, Budapest, Hungary, goda.tibor@bgk.uni-obuda.hu

Abstract

Human locomotion relies on muscle synergies—modular strategies of the central nervous system—yet prior studies on chronic ankle instability (CAI) have largely focused on isolated muscle activation. To elucidate muscle coordination dynamics, we analyzed synergy patterns during landing in 22 unilateral CAI patients and 22 healthy controls. Surface EMG signals from ten muscles were processed using a recursive second-order differential equation model and decomposed via non-negative matrix factorization (NNMF). Four synergies were identified in both groups. CAI patients exhibited significantly higher gluteus maximus weighting in Synergy 1 ($p=0.0035$) and altered vastus lateralis weighting in Synergies 2 ($p=0.018$) and 4 ($p=0.030$). Temporally, Synergy 1 in the CAI group showed reduced activation duration ($p=0.011$) and earlier peak activation ($p=0.01$). While CAI patients retain a modular framework comparable to healthy individuals, specific spatiotemporal adjustments—particularly in the gluteus maximus and vastus lateralis—suggest compensatory strategies and provide novel insights for rehabilitation protocols.

Keywords: Muscle synergy; Non-negative matrix factorization; K-means clustering; Chronic ankle instability

1 Introduction

Lateral ankle sprains are a ubiquitous musculoskeletal injury, accounting for approximately 10–30% of all sports-related traumas [1]. Without timely and effective management, up to 70% of these cases progress to chronic ankle instability (CAI), characterized by recurrent sprains, perceived instability, and significant quality of life impairments [2]. Recent advancements in rehabilitation have consequently shifted focus from purely anatomical interventions to addressing dynamic mechanical and sensorimotor deficits.

Ligamentous injuries in CAI are closely linked to perceptual dysfunction, mediated by reduced gamma motor neuron activation and muscle spindle sensitivity [3]. These physiological alterations impair the reception of mechanical stimuli and proprioceptive feedback, disrupting the sensorimotor loop and leading to aberrant muscle activation. While altered activation patterns in muscles such as the peroneus longus and tibialis anterior suggest a multi-muscle compensatory strategy, the precise neural mechanisms coordinating these adaptations remain unclear [4]. Kinematically, CAI patients exhibit distinct compensatory strategies during landing, such as reduced ankle plantarflexion and increased hip flexion [5]. The former acts as a protective mechanism to limit tension on the lateral ligaments, while the latter reflects a proximal neuromuscular compensation for distal deficits. These alterations suggest that the central nervous system (CNS) redistributes mechanical loads across redundant structures to maintain stability.

To elucidate the neural control underlying these movements, researchers have traditionally relied on surface electromyography (sEMG). However, conventional sEMG analysis is limited to isolated muscle activity, often overlooking the modular organization of motor control. Since the CNS coordinates movement through functional units rather than individual muscles, a synergistic approach is essential for a comprehensive understanding [6]. Muscle synergy analysis, often employing non-negative matrix factorization (NNMF), offers a robust framework to decode these modular control strategies [7]. Although Kim et al. utilized this method to identify altered weighting of the tibialis anterior during cutting tasks in CAI patients, the organization of muscle synergies during landing—a high-risk maneuver for sprains—remains unexplored [8].

Therefore, this study aimed to investigate muscle synergy patterns during landing in individuals with and without CAI. We hypothesized that while the number of synergies would remain conserved in CAI patients, specific muscle weights and temporal activation patterns would be altered to accommodate the biomechanical adaptations necessitated by ankle instability.

2 Methods

As illustrated in Fig. 1, the analytical framework of this study comprised four sequential stages: (1) sEMG acquisition, (2) muscle activation estimation, (3) synergy extraction, and (4) pattern classification.

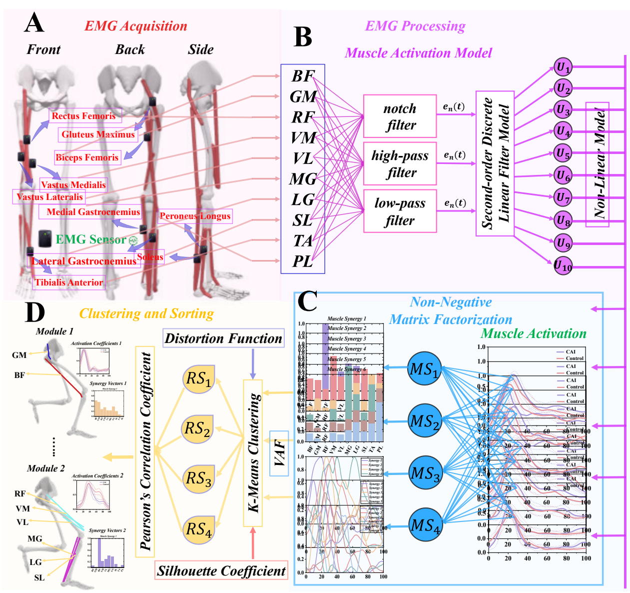

Figure 1. Overview of the overall workflow of the current study. (A) Acquisition of surface electromyographic signals. (B) sEMG signals from ten muscles were used to derive muscle activation using a muscle activation model. (C) Muscle synergy extraction using the NNMF algorithm. (D) Sorting of muscle synergies using K-means clustering algorithm and Pearson's correlation coefficient.

2.1 Participants

A total of 22 patients with unilateral chronic ankle instability (CAI) and 22 healthy controls were recruited for this study. Screening and eligibility were determined in accordance with the International Ankle Consortium (IAC) consensus statement. Inclusion criteria for the CAI group were: (1) a Cumberland Ankle Instability Tool (CAIT) score ≤ 24; (2) a history of traumatic ankle sprain requiring at least two medical consultations; and (3) recurrent episodes of the ankle "giving way" or feelings of instability for at least six months. Conversely, the healthy control group consisted of individuals with no history of lateral ankle sprains and a CAIT score of ≥ 29. Exclusion criteria for both groups included a history of lower extremity fractures, surgeries, or bilateral ankle sprains. To control for the confounding effects of limb dominance, only right-leg dominant participants (defined as the preferred leg for kicking a ball) were recruited, and the dominant limb was the injured side in the CAI group. All participants provided written informed consent after being fully briefed on the study's purpose and procedures.

2.2 Experimental Protocol and Data Recordings

Following the SENIAM guidelines [9], electrode sites were prepared by shaving and cleaning with alcohol to minimize skin-electrode impedance. Ten wireless sEMG sensors (Delsys, Boston, MA, USA) were positioned over the muscle bellies of the soleus (SL), medial gastrocnemius (MG), lateral gastrocnemius (LG), tibialis anterior (TA), peroneus longus (PL), rectus femoris (RF), vastus medialis (VM), vastus lateralis (VL), biceps femoris (BF), and gluteus maximus (GM). Prior to data collection, participants performed a 15-minute dynamic warm-up and familiarized themselves with the single-leg jump-landing task. No feedback on landing technique was provided to preserve natural movement patterns. Participants stood on their involved limb at a standardized distance (equivalent to 100% of their leg length, measured from the greater trochanter to the lateral malleolus) from the landing target. With hands placed on hips to minimize arm-swing influence, participants jumped over a 15-cm hurdle, landed on the same limb, and maintained balance for 5 seconds while looking forward.

All trials were performed barefoot. A successful trial required the participant to land squarely on the target and maintain stability without extraneous movement; otherwise, the trial was repeated. Three successful trials were recorded with 3-minute rest intervals between each. EMG data were sampled at 1000 Hz via the EMGworks system (Delsys, Boston, USA). Raw sEMG signals were processed using a custom pipeline in MATLAB R2022 (MathWorks, Natick, MA, USA). To eliminate artifacts, signals were subjected to a 50Hz notch filter (to remove power-line noise) and a 30Hz zero-phase high-pass filter (to remove motion artifacts). Subsequently, the signals were full-wave rectified and smoothed using a 5Hz zero-phase low-pass filter to generate the linear envelope. The same preprocessing protocol was applied to the maximal voluntary contraction (MVC) trials, and muscle activity was normalized to the peak MVC amplitude. To account for excitation–contraction coupling, muscle activation was estimated using a second-order recursive filtering model incorporating a 10ms electromechanical delay [10]. Model stability was ensured via fixed recursive coefficients, and a non-linear excitation–activation transformation (shape coefficient=1.5) was applied to simulate physiological activation characteristics [11]. Finally, all activation waveforms were time-normalized to 101 points, representing 0–100% of the landing phase.

2.3 Muscle Synergy Pattern Extraction

Non-negative Matrix Factorization (NNMF) was applied to the processed muscle activation matrices to extract two components: synergy vectors, representing spatial coordination patterns, and activation coefficients, capturing temporal dynamics [12]. The decomposition was solved via a multiplicative update algorithm within an iterative gradient framework, minimizing the Euclidean reconstruction error. The optimal number of synergies was determined based on the Variance Accounted For (VAF). Consistent with established criteria, the minimal number of synergies was selected when the global VAF exceeded 90% and the VAF for each individual muscle exceeded 75% [13]. To identify canonical motor modules, synergy vectors from the healthy group were concatenated and clustered using the K-means++ algorithm. The resulting centroids served as reference modules. Synergies from all experimental trials were subsequently matched to these reference modules based on the highest Pearson correlation coefficients. All computational analyses were performed in MATLAB R2022 using the built-in NNMF and kmeans functions.

2.4 Statistical Analysis

Statistical analyses were performed using MATLAB R2022. The normality of data distribution and homogeneity of variances were assessed using the Shapiro-Wilk test and Levene's test, respectively. For discrete variables (e.g., muscle weights, peak coefficients), between-group differences were evaluated using independent samples t-tests. If the assumptions of normality or homogeneity were violated, the non-parametric Wilcoxon rank-sum test was employed. The significance level was set at alpha=0.05. Effect sizes were quantified using Cohen's d to assess the magnitude of differences, with thresholds defined as: small ($0.2<d<0.5$), medium ($0.5<d<0.8$), and large ($d\geqslant 0.8$). To examine temporal differences in activation patterns throughout the landing phase, Statistical Parametric Mapping (SPM) was utilized [14]. SPM allows for the comparison of continuous field data (1D time-series) rather than discrete points. The critical threshold was calculated based on Random Field Theory (RFT). Significant differences were identified where the SPM trajectory crossed this critical threshold.

3 Results

3.1 Number of Muscle Synergies Extraction by NNMF

According to predefined criteria for the optimal number of muscle synergies for each group in various conditions, we observed that the neuromotor organization of most CAI patients and healthy controls during landing could be characterized by 4-6 muscle synergy patterns. To enhance clarity in our presentation, we depict the synergy vectors matrix and activation coefficient matrix for only the four extracted muscle synergies from each subject group (Fig. 2, Fig. 3).

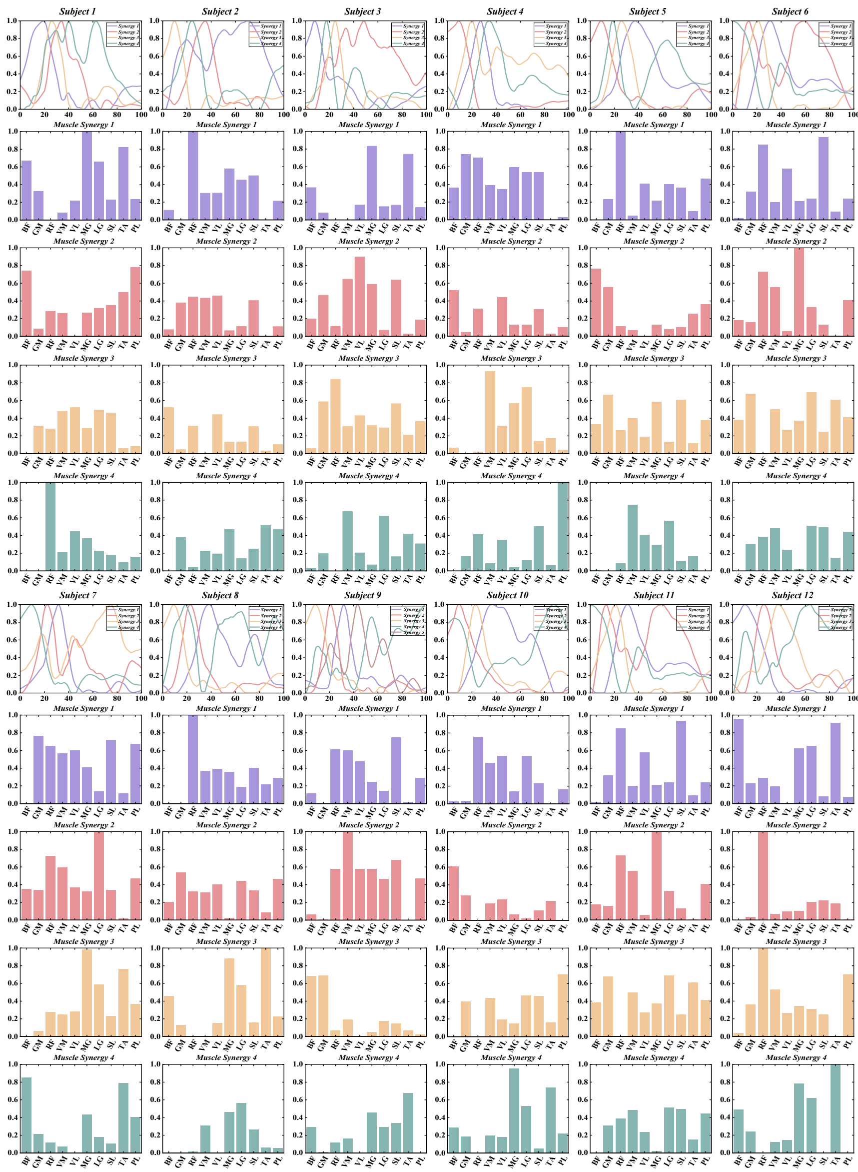

Figure 2. The extracted synergy vectors matrix and activation coefficient matrix from 12 subjects in the CAI group are presented, with activation coefficient results displayed in rows 1 and 6, and the remaining rows depicting the synergy vectors.

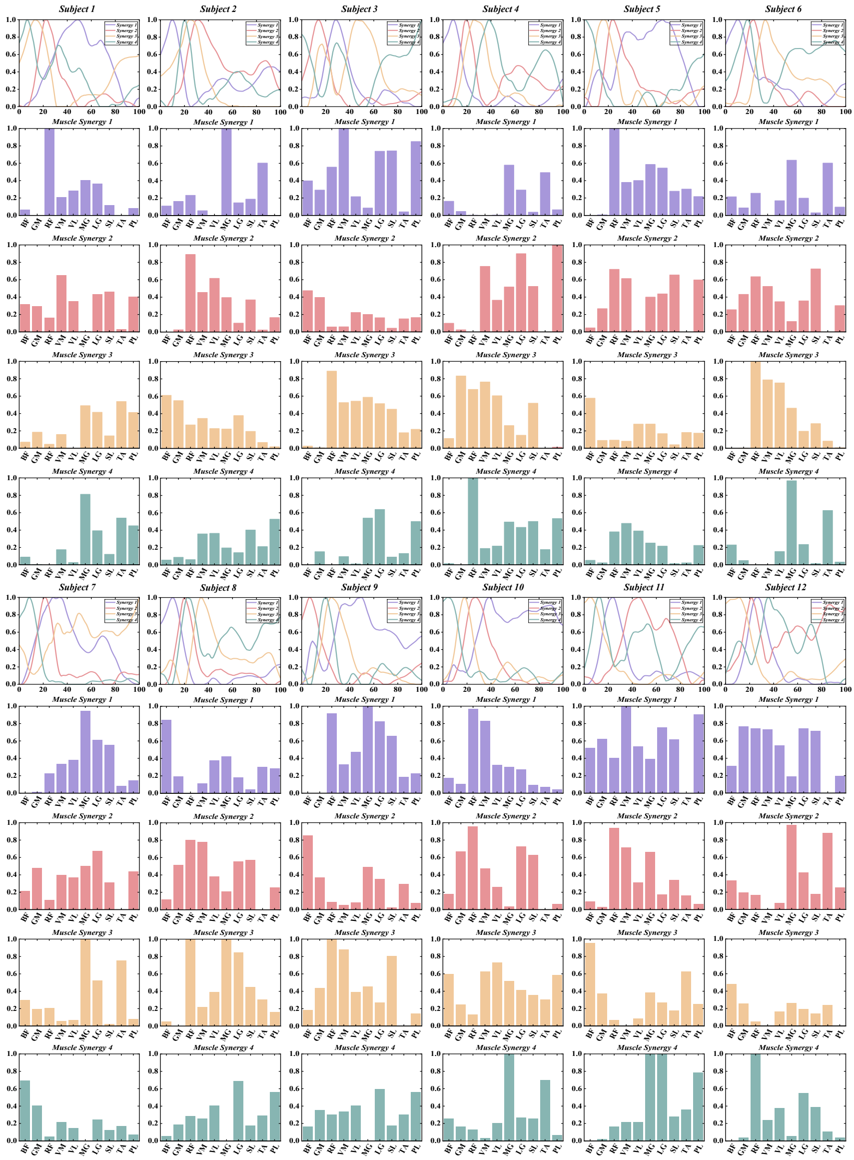

Figure 3. The extracted synergy vectors matrix and activation coefficient matrix from 12 subjects in the healthy group are presented, with activation coefficient results displayed in rows 1 and 6, and the remaining rows depicting the synergy vectors.

In most cases, with four muscle synergies, both the CAI and healthy groups achieved global VAF above 90% and local muscle VAFs exceeding 75% (Fig. 4). No statistically significant differences were observed between the CAI and healthy groups regarding the number of muscle synergies, global VAF, and local muscle VAF (Fig. 4).

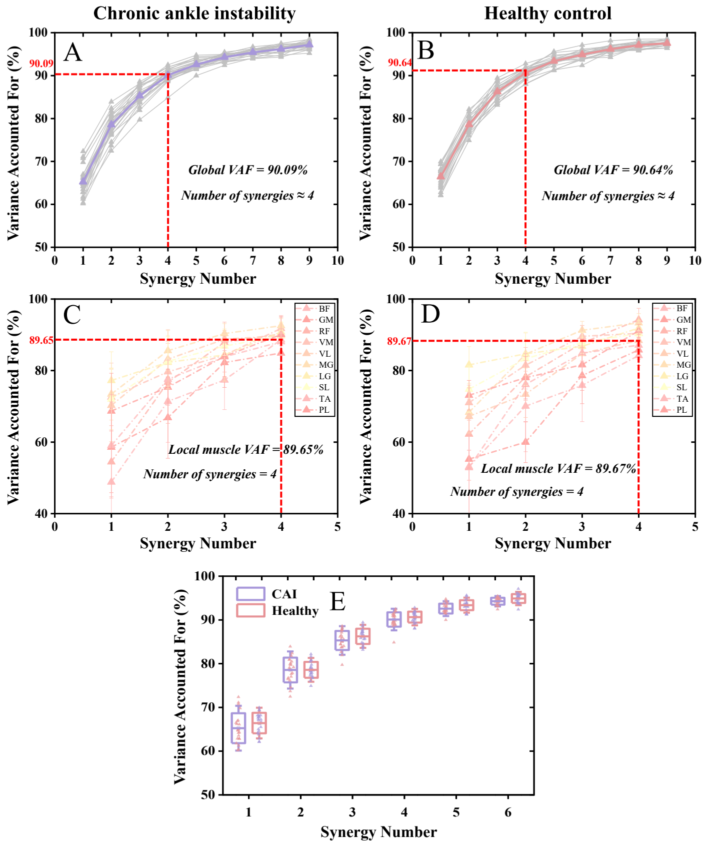

Figure 4. Global and local muscle VAFs. (A) The global VAF corresponding to each synergy in the CAI group. (B) The global VAF corresponding to each synergy in the healthy group. (C) The local muscle VAF corresponding to each synergy in the CAI group. (D) The local muscle VAF corresponding to each synergy in the healthy group. (E) Comparison of global VAF corresponding to muscle synergies 1-6 in the CAI and healthy groups.

3.2 Characteristics of Temporal and Spatial Modules.

In Synergy 1, there were no statistically significant differences in most of the muscle-specific relative weights, with only the GM showing a significantly higher relative weight ($p = 0.0035$, $d = 0.903$) in the in the CAI group compared with the healthy controls. As for Synergy 2, relative weights of the GM and PL were significantly higher in CAI ($p = 0.042$, $d = 0.852$, $p = 0.006$, $d = 0.910$, respectively), while healthy controls showed significantly higher relative weights for the VL and LG ($p = 0.018$, $d = 0.800$, $p = 0.049$, $d = 0.665$, respectively), which are muscles that exhibited heightened activity within the corresponding motor module. Within Synergy 3, CAI exhibited significantly higher relative weights of the BF and the TA ($p = 0.026$, $d = 0.929$, $p = 0.042$, $d = 0.595$, respectively), while the BF displaying diminished contribution to the corresponding functional module and remaining inactive. For Synergy 4, CAI demonstrated significantly higher relative weights of the VL compared to healthy ($p = 0.030$, $d = 0.873$). Conversely, the relative weights of the BF, LG, and PL were significantly lower in CAI than in healthy ($p = 0.002$, $d = 1.196$, $p = 0.005$, $d = 1.274$, $p = 0.047$, $d = 0.863$, respectively). No significant differences in relative weights of other muscles were observed. The SPM1d results revealed significant differences in activation coefficient only within Synergy 3, notably between 51% and 81% of the landing phase ($p < 0.001$), with significantly higher amplitude observed in CAI compared to healthy controls. Other muscle synergies exhibited comparable activation coefficient profiles (Fig. 5).

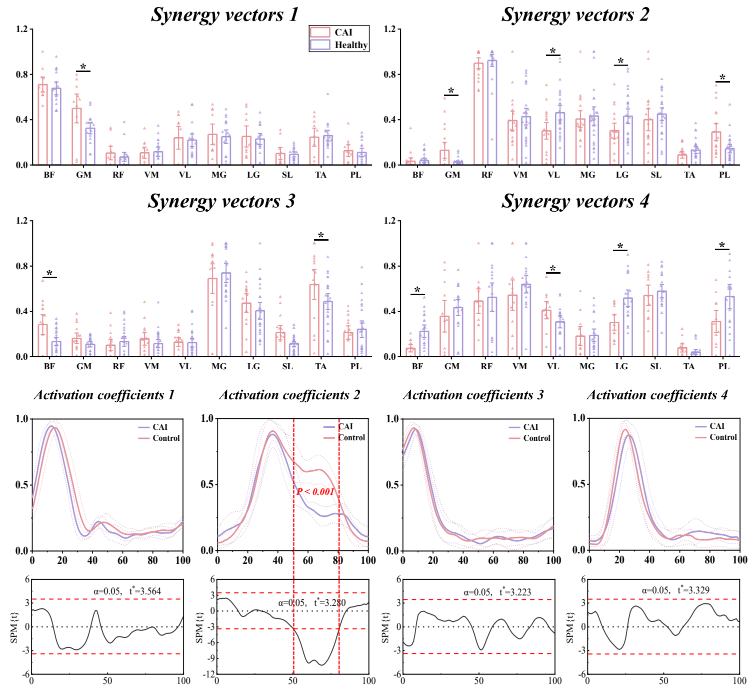

*Figure 5. The synergy vectors, activation coefficients, and SPM1d results for activation coefficients in the muscle synergies extracted from each group. *: significant difference with p < 0.05.*

4 Discussion

This study represents the first detailed quantification of neuromotor modular organization in patients with CAI during landing. Consistent with our hypothesis, the number of muscle synergies remained conserved between groups, suggesting a similar modular complexity. However, CAI patients demonstrated significant reorganization in muscle-specific weights and temporal activation patterns. These adaptations highlight a shift in control strategy: a reliance on proximal hip regulation, compromised knee coordination, and cautious ankle stabilization.

The Hip Strategy (Synergy 1) A primary finding was the enhanced recruitment and earlier peak activation of the gluteus maximus (GM) in CAI patients. This aligns with the "proximal compensation" hypothesis [15], where neuromuscular control shifts from the unstable distal joint to the proximal hip to maintain postural equilibrium. The shortened time-to-peak activation suggests a feed-forward mechanism to mitigate excessive internal femoral rotation during initial contact, thereby optimizing lower limb alignment and reducing injury risk [16]. Thus, the GM serves as a critical pivotal point for stability in CAI populations.

The Knee Strategy (Synergy 2) CAI patients exhibited impaired knee control strategies, characterized by reduced activation duration and amplitude in the vastus lateralis (VL) and gastrocnemius. Since the ankle acts as the primary shock absorber during landing [17], ankle dysfunction likely necessitates altered knee mechanics. Our results corroborate previous studies showing reduced knee flexion and cushioning capacity in CAI, which may inadvertently increase vertical ground reaction forces and the risk of proximal injuries, including ACL tears [18]. The altered spatiotemporal parameters in this module suggest that proprioceptive deficits hinder the effective recruitment of knee stabilizers.

The Ankle Strategy (Synergy 3) Regarding ankle control, CAI patients displayed increased Tibialis Anterior (TA) contribution with a delayed peak activation. While some literature suggests increased dorsiflexion is a protective self-preservation mechanism [19], excessive TA recruitment can compromise frontal plane stability. The observed delayed peak likely represents a refined neuromotor response: patients attempt to utilize the TA for stability while modulating recruitment timing to prevent excessive rigidity or instability during the critical impact phase. Global Integration and Adaptation (Synergy 4) In the multi-joint coordination module (Synergy 4), we observed a trade-off: reduced contributions from the lateral gastrocnemius and peroneus longus, but adaptive increases in VL weighting. The reduction in peroneus longus activity may compromise the foot's ability to withstand lateral loading, elevating re-injury risk. However, the compensatory increase in VL weighting suggests the central nervous system (CNS) prioritizes knee extensor robustness to counteract lateral forces and limit excessive sway. This highlights a complex reorganization where the CNS sacrifices some distal control for proximal robustness.

This study has limitations. First, the recruitment of only male participants limits generalizability to females, who may exhibit distinct landing biomechanics. Second, despite filtering, surface EMG is susceptible to crosstalk from adjacent muscles. Finally, the absence of synchronous kinematic and kinetic data precludes a direct correlation between internal motor drive and external biomechanical outcomes.

5 Conclusion

This study systematically explored muscle synergy patterns during landing in individuals with Chronic Ankle Instability (CAI). By employing NNMF decomposition and K-means clustering, we identified distinct neuromuscular control strategies characteristic of this population. Our findings indicate that CAI patients adapt to ankle instability by modulating both the spatial and temporal components of specific motor modules, with prominent alterations observed in the gluteus maximus and tibialis anterior. Furthermore, while general deficits were noted in the knee control module, the compensatory adjustments of the vastus lateralis across different synergies highlight a complex reorganization strategy. These insights provide a refined biomechanical basis for developing targeted rehabilitation protocols that look beyond the ankle to address proximal and multi-joint deficits.

6 References

[1] Hølmer P, Søndergaard L, Konradsen L, Nielsen PT, & Jørgensen LN (1994) Epidemiology of sprains in the lateral ankle and foot. Foot & ankle international 15(2):72-74.

[2] Wikstrom EA, Hubbard-Turner T, & McKeon PO (2013) Understanding and treating lateral ankle sprains and their consequences: a constraints-based approach. Sports medicine 43(6):385-393.

[3] Thompson C, et al. (2018) Factors contributing to chronic ankle instability: a systematic review and meta-analysis of systematic reviews. Sports Medicine 48(1):189-205.

[4] Son SJ, Kim H, Seeley MK, & Hopkins JT (2017) Movement Strategies among Groups of Chronic Ankle Instability, Coper, and Control. Medicine and science in sports and exercise

49(8):1649-1661.

[5] Jie T, et al. (2024) Structural and organizational strategies of locomotor modules during landing in patients with chronic ankle instability. Bioengineering 11(5):518.

[6] Kerkman JN, Daffertshofer A, Gollo LL, Breakspear M, & Boonstra TW (2018) Network structure of the human musculoskeletal system shapes neural interactions on multiple time scales. Science advances 4(6):eaat0497.

[7] Lee DD & Seung HS (1999) Learning the parts of objects by non-negative matrix factorization. nature 401(6755):788-791.

[8] Kim H, Palmieri-Smith R, & Kipp K (2023) Muscle synergies in people with chronic ankle instability during anticipated and unanticipated landing-cutting tasks. Journal of Athletic Training 58(2):143-152.

[9] Stegeman D & Hermens H (2007) Standards for surface electromyography: The European project Surface EMG for non-invasive assessment of muscles (SENIAM). Enschede: Roessingh Research and Development 10(8).

[10] Buchanan TS, Lloyd DG, Manal K, & Besier TF (2004) Neuromusculoskeletal modeling: estimation of muscle forces and joint moments and movements from measurements of neural command. Journal of applied biomechanics 20(4):367-395.

[11] Van Ruijven L & Weijs W (1990) A new model for calculating muscle forces from electromyograms. European journal of applied physiology and occupational physiology 61(5):479-485.

[12] Lee D & Seung HS (2000) Algorithms for non-negative matrix factorization. Advances in neural information processing systems 13.

[13] Choi Y, Kim Y, Kim M, & Yoon B (2019) Muscle synergies for turning during human walking. Journal of motor behavior 51(1):1-9.

[14] Pataky TC (2012) One-dimensional statistical parametric mapping in Python. Computer methods in biomechanics and biomedical engineering 15(3):295-301.

[15] Jie T, et al. (2025) Muscle mechanics and energetics in chronic ankle instability and copers during landing: Strategies for adaptive adjustments in locomotion pattern. Heliyon 11(2).

[16] Feger MA, Donovan L, Hart JM, & Hertel J (2015) Lower extremity muscle activation in patients with or without chronic ankle instability during walking. Journal of athletic training 50(4):350-357.

[17] Yeow CH, Lee PVS, & Goh JCH (2011) An investigation of lower extremity energy dissipation strategies during single-leg and double-leg landing based on sagittal and frontal plane biomechanics. Human movement science 30(3):624-635.

[18] Gribble P & Robinson R (2010) Differences in spatiotemporal landing variables during a dynamic stability task in subjects with CAI. Scandinavian journal of medicine & science in sports 20(1):e63-e71.

[19] Wright CJ, Arnold BL, & Ross SE (2016) Altered kinematics and time to stabilization during drop-jump landings in individuals with or without functional ankle instability. Journal of athletic training 51(1):5-15.